13th International Conference on Applied Electromagnetics - ΠΕC 2017
August 30 – September 01, 2017, Niš, Serbia

NUMERICAL ANALYSIS OF TRANSIENT AND STEADY-STATE OPERATION OF THREE-PHASE INDUCTION MOTOR

Vasilija SARAC[1], Goce STEFANOV[2]

Abstract: Paper presents two mathematical models derived in order to obtain transient performance characteristics of three-phase induction motor. First model is suitable for application in Simulink under Matlab and consequently the set of differential equation, which define motor transient characteristics under different operating modes, are solved in Simulink. Second model and its set of differential equation are solved using numerical methods in Matlab. Finite Element Method is applied as numerical method for calculation of magnetic flux density in motor cross-section for different operating modes.

Keywords: Finite element method, flux density distribution, three-phase induction motor, transient characteristics.

INTRODUCTION

Three phase induction asynchronous motors are one of the mostly widespread induction motors in industrial applications. They are robust, reliable with relatively low maintenance costs. Assessment of their coupling with the load and their behavior during start-up as well as during steady state operating is one of the most important engineering tasks. Transient models of the machines giving dynamic characteristics of various variables, associated with machine operation such as: speed, torque or currents are valuable tools in assessment of the machine operation at different operating regimes (no-load, rated load or locked-rotor operation [1]-[4]. Usually these models are based on one general transformation, which eliminates all time-varying inductances in the electrical machine by referring the stator and rotor variables to a frame of reference, which may rotate at any angular velocity or remain stationary. All known transformations may be obtained by the simple assigning of the appropriate speed of rotation to this so-call arbitrary reference frame [5]. Two different mathematical models are derived for obtaining transient characteristics. First model is defined with set of five differential equations of first order derived and modified in order to be applicable for solving in Simulik. This model is referred as simulation model (SM). Reference frame theory is applied in this mathematical model in synchronously rotating reference frame. Second model is defined with another set of five differential equations of first order derived in stationary reference frame. They are solved in Matlab by using method of Runge Kutta of fourth order. This model is referred as numerical model (NM). Motor speed and electromagnetic torque as time-dependent variables are obtained from both motor models. Obtained results are compared for two operating modes: no-load and rated load as they are considered to be the most important operating modes of the motor. Finally results from the both models are compared with available data from measurements in order their accuracy to be verified. Estimation of motor operation at various loads via magnetic flux density distribution in motor cross-section is analyzed by the aid of numerical technique Finite Element Method (FEM). Numerical methods are also used in design of induction motors [6]. They provide a valuable information about points of core saturation at various operating modes, allowing improvement of motor construction. In this paper three phase squirrel cage asynchronous motor with rated data: power 2.2kW, speed 1410rpm, voltage 220/380V and current 8.7/5A is analyzed.

TRANSIENT MOTOR MODELS

Simulation model

Transformation of three-phase variables associated to stator circuit of the motor (a, b, c) into arbitrary rotating reference frame (d, q) in general case is done by:

$$\mathbf{f}_{qd0s} = \mathbf{K}_s \mathbf{f}_{abcs} \tag{1}$$

$$\left(\mathbf{f}_{qd0s}\right)^T = \left[f_{qs} f_{ds} f_{0s}\right] \tag{2}$$

$$\left(\mathbf{f}_{abcs}\right)^T = \left[f_{as} f_{bs} f_{cs}\right]. \tag{3}$$

Transformation matrix is:

$$\mathbf{K}_s = \frac{2}{3}\begin{bmatrix} \cos\theta & \cos\left(\theta - \frac{2\pi}{3}\right) & \cos\left(\theta + \frac{2\pi}{3}\right) \\ \sin\theta & \sin\left(\theta - \frac{2\pi}{3}\right) & \sin\left(\theta + \frac{2\pi}{3}\right) \\ \frac{1}{2} & \frac{1}{2} & \frac{1}{2} \end{bmatrix}. \tag{4}$$

Angular displacement θ is defined as:

$$\theta = \int_0^t \omega(\xi) d\xi + \theta(0), \tag{5}$$

where ξ is dummy variable of integration.

In (2) and (3) variable f can represent voltages, currents and fluxes of stator winding. Subscript "*s*" denotes the variables, parameters and transformations associated to the stator circuits. Angular displacement θ must be continuous, but the angular velocity associated to the change of variables is unspecified. First step in mathematical modeling of transi-

[1] University "Goce Delcev", Faculty of Electrical Engineering, P.O. Box 201, 2000 Stip, Macedonia, e-mail: vasilija.sarac@ugd.edu.mk
[2] University "Goce Delcev", Faculty of Electrical Engineering, P.O. Box 201, 2000 Stip, Macedonia, e-maill: goce.stefanov@ugd.edu.mk

ent motor model in Simulink is to transform the supply voltages from three-phase system (a, b, c) into synchronously rotating d, q system. Transformation equations are:

$$U_{ds} = -\frac{1}{\sqrt{3}}\left(U_b - U_c\right)\cos\theta + U_a \sin\theta \tag{6}$$

$$U_{qs} = \frac{1}{\sqrt{3}}\left(U_b - U_c\right)\sin\theta + U_a \cos\theta, \tag{7}$$

where $\omega = \frac{d\theta}{dt}$ i.e. $\theta = \int_0^t \omega dt$. Voltage U_a, U_b and U_c are three phase supply voltages at 220V, 50Hz. Variable ω is associated to the frequency of the supply voltage of the motor. In case of symmetrical three-phase supply voltage ω=314rad/s. Voltage equations of the stator and rotor circuits are:

$$U_{qs} = R_s i_{qs} + \omega \psi_{ds} + \frac{d\psi_{qs}}{dt} \tag{8}$$

$$U_{ds} = R_s i_{ds} - \omega \psi_{qs} + \frac{d\psi_{ds}}{dt} \tag{9}$$

$$0 = R_r i_{qr} + (\omega - \omega_r)\psi_{dr} + \frac{d\psi_{qr}}{dt} \tag{10}$$

$$0 = R_r i_{dr} - (\omega - \omega_r)\psi_{qr} + \frac{d\psi_{dr}}{dt}. \tag{11}$$

In (10) and (11) transformed rotor voltages U_{qr} and U_{dr} are considered to be equal to zero, since the rotor winding is squirrel cage type and consequently it is short circuited. In above equations ω_r is the rotor angular velocity and ω is arbitrary angular speed, which depends on the frequency of the voltage supply. Flux linkages of stator and rotor circuits are defined as:

$$\psi_{qs} = L_s i_{qs} + L_{sr} i_{qr} \tag{12}$$

$$\psi_{ds} = L_s i_{ds} + L_{sr} i_{dr} \tag{13}$$

$$\psi_{qr} = L_r i_{qr} + L_{sr} i_{qs} \tag{14}$$

$$\psi_{dr} = L_r i_{dr} + L_{sr} i_{ds}. \tag{15}$$

All variables associated with stator have subscript "*s*" and those ones associated with rotor have subscript "*r*". R_s and R_r are the stator and rotor resistance, L_s and L_r are stator and rotor inductances and L_{sr} is the mutual inductance between stator and rotor winding. By expressing the stator currents i_{qs} and i_{ds} from (12) and (13) and their replacement into (14) and (15) following equations are obtained:

$$\psi_{qr} = L_r i_{qr} + L_{sr}\left(\frac{\psi_{qs}}{L_s} - \frac{L_{sr}}{L_s} i_{qr}\right) \tag{16}$$

$$\psi_{dr} = L_r i_{dr} + L_{sr}\left(\frac{\psi_{ds}}{L_s} - \frac{L_{sr}}{L_s} i_{dr}\right). \tag{17}$$

By replacing (16) and (17) into (10) and (11) and integrating over the time:

$$i_{qr} = \frac{L_s R_r}{L_{sr}^2 - L_s L_r}\int_0^t i_{qr} dt - \omega \int_0^t i_{dr} dt + \frac{L_{sr}\omega}{L_{sr}^2 - L_s L_r}\int_0^t \psi_{ds} dt + \int_0^t \omega_r i_{dr} dt - \frac{L_{sr}}{L_{sr}^2 - L_s L_r}\int_0^t \omega_r \psi_{ds} dt + \frac{L_{sr}}{L_{sr}^2 - L_s L_r}\psi_{qs} \tag{18}$$

$$i_{dr} = \frac{L_s R_r}{L_{sr}^2 - L_s L_r}\int_0^t i_{dr} dt + \omega \int_0^t i_{qr} dt - \frac{L_{sr}\omega}{L_{sr}^2 - L_s L_r}\int_0^t \psi_{qs} dt - \int_0^t \omega_r i_{qr} dt + \frac{L_{sr}}{L_{sr}^2 - L_s L_r}\int_0^t \omega_r \psi_{qs} dt + \frac{L_{sr}}{L_{sr}^2 - L_s L_r}\psi_{ds}. \tag{19}$$

Flux linkages ψ_{ds} and ψ_{qs} can be expressed from transformed voltages U_{ds} and U_{qs}. By replacing currents i_{qs} and i_{ds} in (10), (11), and rearranging the equations per flux linkages and their integration over the time:

$$\psi_{qs} = \int_0^t U_{qs} dt - \frac{R_s}{L_s}\int_0^t \psi_{qs} dt + \frac{L_{sr} R_s}{L_s}\int_0^t i_{qr} dt - \omega \int_0^t \psi_{ds} dt \tag{20}$$

$$\psi_{ds} = \int_0^t U_{ds} dt - \frac{R_s}{L_s}\int_0^t \psi_{ds} dt + \frac{L_{sr} R_s}{L_s}\int_0^t i_{dr} dt + \omega \int_0^t \psi_{qs} dt. \tag{21}$$

Equations (6), (7), (18), (19), (20) and (21) together with equation, which defines the rotor speed, are part of the motor transient model. Equation of rotor speed is:

$$\omega_r = \frac{6L_{sr}}{JL_s}\int_0^t \psi_{qs} i_{dr} dt - \frac{6L_{sr}}{JL_s}\int_0^t \psi_{ds} i_{qr} dt - \frac{2}{J}\int_0^t M_s dt. \tag{22}$$

M_s [Nm] is the load torque and J [kgm^2] is the moment of inertia of the motor. Rotor currents and flux linkages are expressed with integral equations instead of differential as in this case Simulink has more stability in convergence of the solution when equations are expressed in integral form. Electromagnetic torque is found from:

$$M_{em} = \left(\frac{3}{2}\right)\left(\frac{P}{2}\right)L_{sr}\left(\frac{\psi_{qs}}{L_s} i_{dr} - \frac{\psi_{ds}}{L_s} i_{qr}\right). \tag{23}$$

P is the number of poles of the motor. The presented equations (6), (7), (18), (19), (20), (21), (22) and (23) are solved in Simulink for Matlab. As an output results electromagnetic torque and rotor speed as time dependant variables are obtained from the simulation model for two different operating regimes: no-load and rated load. In order, accuracy of the developed mathematical model to be verified second transient model of the motor is constructed with set of five differential equations, where motor variables are transformed into stationary frame of reference. The equations are solved in Matlab with Runge Kutta solver of forth order (numerical model).

Numerical model

Motor numerical model is consisted of set of five differential equations in which time-dependant variables (flux linkages and speed) are transformed in the stationary reference frame or α, β reference frame. Differential equations are:

$$\frac{d\psi_{s\alpha}}{dt} = \sqrt{2}U_{nf}\cos\omega t - a_1\psi_{s\alpha} + a_2\psi_{r\alpha} \quad (24)$$

$$\frac{d\psi_{s\beta}}{dt} = \sqrt{2}U_{nf}\cos\omega t - a_1\psi_{s\beta} + a_2\psi_{r\beta} \quad (25)$$

$$\frac{d\psi_{r\alpha}}{dt} = a_3\psi_{s\alpha} - a_4\psi_{r\alpha} - \omega_r\psi_{r\beta} \quad (26)$$

$$\frac{d\psi_{r\beta}}{dt} = a_3\psi_{s\beta} - a_4\psi_{r\beta} + \omega_r\psi_{r\alpha} \quad (27)$$

$$\frac{d\omega_r}{dt} = P\left(M_{em} - M_s\right)/J \quad (28)$$

$$M_{em} = a_5\left(\psi_{s\beta}\psi_{r\alpha} - \psi_{r\beta}\psi_{s\alpha}\right) \quad (29)$$

$$a_1 = \frac{R_s L_r}{L_s L_r - L_{sr}^2};\ a_2 = \frac{R_s L_{sr}}{L_s L_r - L_{sr}^2};\ a_3 = \frac{R_r L_s}{L_s L_r - L_{sr}^2};$$

$$a_4 = \frac{R_r L_{sr}}{L_s L_r - L_{sr}^2};\ a_5 = \frac{P L_{sr}}{L_s L_r - L_{sr}^2}$$

Differential equations are solved within defined time interval and in this case, it is one second and for defined starting conditions, (starting values of the flux linkages – ψ). Again, electromagnetic torque – M_{em} and motor speed – ω_r are obtained as output results from motor numerical model.

OUTPUT RESULTS AND DISCUSSIONS

Three-phase squirrel cage motor is analyzed with both motor transient models. Electromagnetic torque and motor speed as time dependent variables are obtained from both motor models. They are calculated for different operating regimes no load and rated load. In Fig. 1 is presented transient performance characteristic of motor speed at no-load from simulation and numerical model. In Fig. 2 is presented electromagnetic torque from both motor models at no-load.

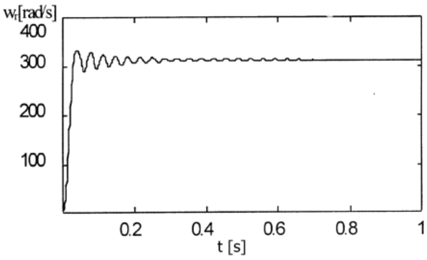

(a) simulation model

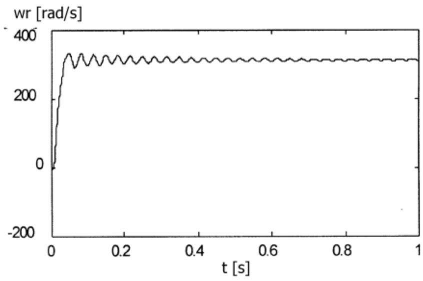

(b) numerical model

Fig. 1 - *Transient characteristic of speed at no-load.*

From presented results in Figs. 1 and 2 it is evident that transient characteristics from both models have the similar waveforms, maximal and steady state values. Acceleration time of the motor is short (less than 0.01 seconds) in both models as motor accelerates without any load. After it is finished motor reaches the steady-state speed of 312rad/s in simulation model and 311rad/s in numerical model, which is in good agreement with measured speed of 313rad/s at no-load operation.

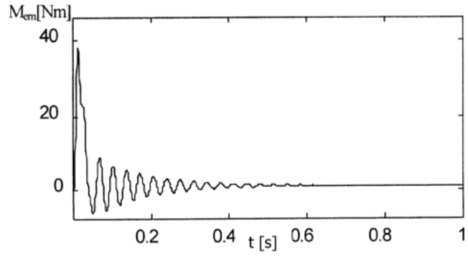

(a) simulation model

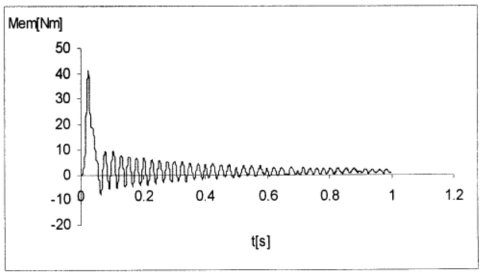

(b) numerical model

Fig. 2 - *Transient characteristic of torque at no-load.*

As for the electromagnetic torque at no-load in the simulation model, it has the steady-state value of 1Nm, in numerical model 1.4Nm and the calculated value is 1.25Nm. In Fig. 3 and 4 are presented characteristics of speed and electromagnetic torque at rated load or acceleration of the motor with load torque of 14Nm.

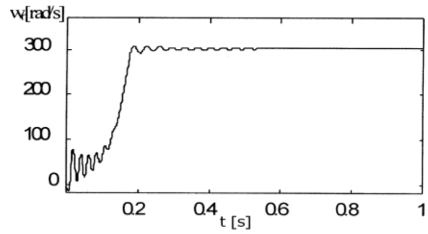

(a) simulation model

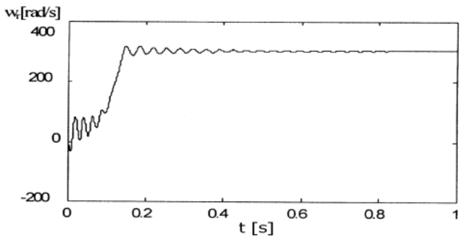

(b) numerical model

Fig. 3 - *Transient characteristic of speed at rated load.*

From Fig. 3 it is evident that motor acceleration time is longer compared to Fig. 1, which is comprehensible, since motor accelerates with load of 14Nm coupled to the motor shaft. After acceleration has finished motor has the steady state value of speed of 303rad/s in numerical model, 301rad/s in simulation model and from the measurement, the rated speed is 295rpm. After acceleration has finished electromagnetic torque in numerical model is 14.6Nm, in simulation model 16,5Nm and calculated value is 15.8Nm.

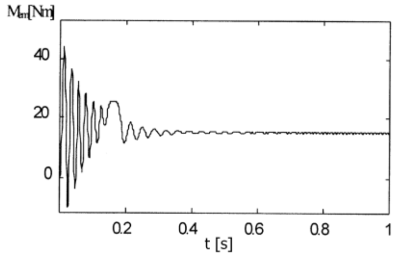

(a) simulation model

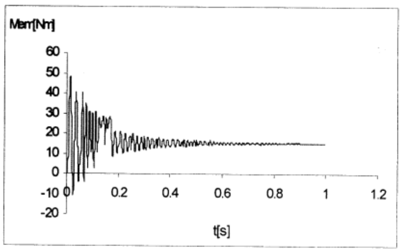

(b) numerical model

Fig. 4- *Transient characteristic of torque at rated load.*

FEM MOTOR MODELS

Finite Element Method (FEM) is a valuable tool in assessment of motor performance and design characteristics. Often some parts of the motor cross-section are exposed to high values of flux density that causes saturation of the motor core, i.e. increased motor losses and operational temperature. Therefore, the motor FEM model has been constructed for two different operating modes: no-load and rated load. The magnetic flux density distribution for mentioned operating modes is presented in Fig. 5.

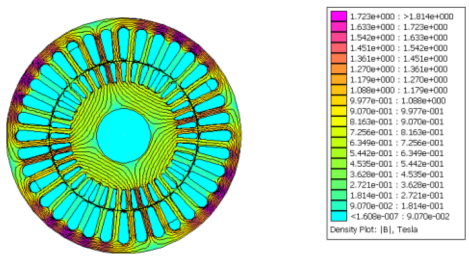

(a) no-load

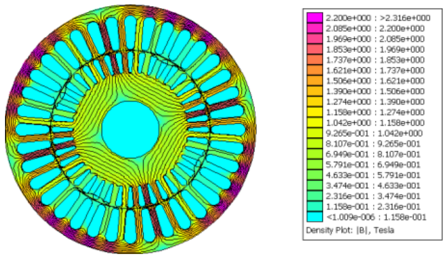

(a) rated-load

Fig. 5 - *Magnetic flux distribution at motor cross-section.*

Magnetic flux density in some points of the motor cross-section at rated load has increased values near to the point of core saturation. Therefore magnetic materials with high quality should be used in order to decrease overall flux density at rated load in motor cross-section. Fig. 6 presents the magnetic flux density in motor air gap at rated load. Obtained value of the flux density in the air gap by FEM confirms the assumed average value of 0.8T in motor analytical model.

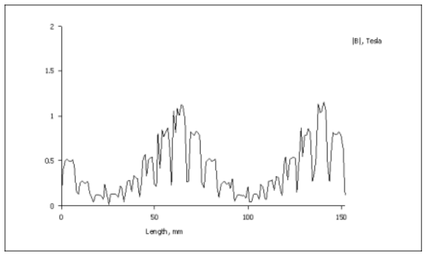

Fig. 6 - *Magnetic flux distribution in motor air gap at rated load.*

CONCLUSION

Dynamic regimes of the inductions motors are not easily estimated especially when motors are coupled with load. Transient models of the machines developed in different software programs enable accurate analysis of motor start-up and steady-state operation in different operating modes. Two transient mathematical models of the induction motor are derived based on machine d, q reference frame theory and solved in two different software: Simulink and Matlab. Output results of motor speed and electromagnetic torque from two models have good agreement. Their accuracy is verified with measurements and analytical calculations as well. Developed models are universal and can be easily altered and applied for any three-phase asynchronous motor supplied with 220V, 50Hz by entering adequate motor parameters. They enable accurate assessment of coupling of the motor with the load thus providing useful data regarding effectives of the complete drive system. Simulink model can be further expanded for different power supplies and frequencies enabling coupling of the motor with the inverter and further expand of its usage in variable speed drives.

REFERENCES

[1] G. Orlovskis, M. Konuhova, K. Ketners: "Comparison of induction motor transient processes characteristics obtained experimentally with those obtained by means of Fortran and Matlab software", Scientific journal of Riga technical university-power and electrical eng., Vol. 29, 2011, pp. 58-62.

[2] K. Makowski, M.J. Wilk.: "Experimental verification of field-circuit model of a single-phase capacitor induction motor", Prezglad electrotechniczny, Vol. 88, No. 7b, 2012, pp. 116-118.

[3] R. Renkeviciene, A. Baskys, A. Petrovas: "Model for simulation of dynamic characteristics of the system frequency converter – AC induction motor", Elektronika ir electrotechnika, Vol.82, No.2, 2008, pp. 65-68.

[4] S.A. Fellag: "Steady state and dynamic evaluation of electrical shaft system", Journal of electrical engineering, Vol. 61, No.5, 2010, pp. 277-281.

[5] R. Bojoi, E. Levi, F. Farina, A. Tenconi, F. Profumo, "Dual three-phase induction motor drive with digital control in stationary reference frame", IEEE Proceedings – Electric power applications, Vol. 153, No. 1, 2006, pp. 129-139.

[6] B.D. Varaticeanu, P. Minnciunescu, D. Fodorean: "Mechanical design and analysis of permanent magnet rotors used in high speed synchronous motor", Electrotechnica, electronica, automatica, Vol. 62, No.1, 2014, pp. 9-17.